

Supporting Information

Dynamics of methylated cytosine flipping by UHRF1

Vasyl Kilin,[†] Krishna Gavvala,[†] Nicolas P.F. Barthes,[‡] Benoît Y. Michel,[‡] Dongwon Shin,[⊥] Christian Boudier,[†] Olivier Mauffret,[#] Valeriy Yashchuk,^h Marc Mousli,[†] Marc Ruff,^{||} Florence Granger,^{||} Sylvia Eiler,^{||} Christian Bronner,^{||} Yitzhak Tor,[§] Alain Burger,[‡] Yves Mély,^{*,†}

Thermal denaturation measurements

The melting curves were monitored by the absorbance changes at 260 nm and converted into a plot of α versus temperature, where α represents the fraction of strands in the duplex state. The melting temperatures were extracted by fitting the first derivative of these curves by a Gaussian (Table S1 and S2).

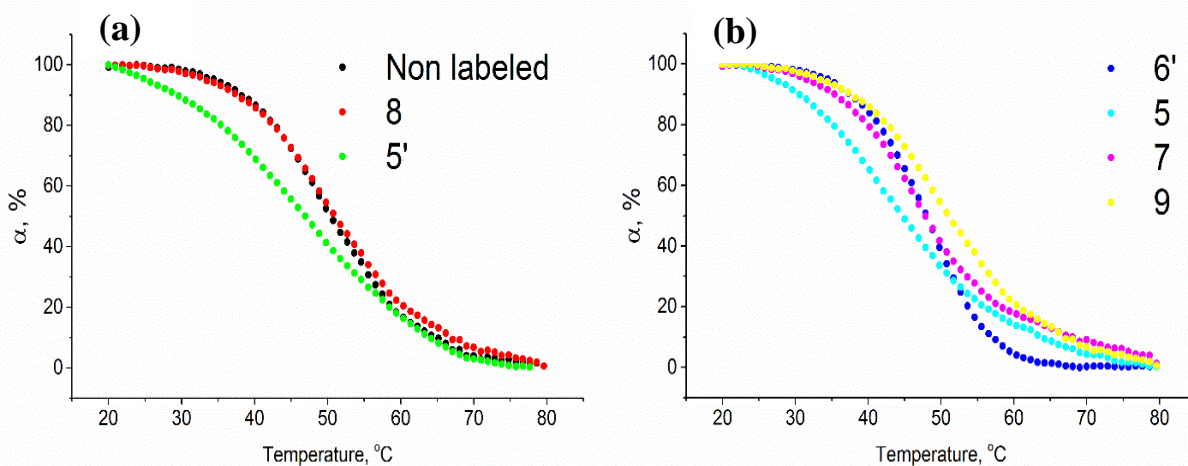


Figure S1. Thermal denaturation curves of 3HCnt-labeled duplexes. The curves are expressed in fraction α of strands in the duplex state versus temperature for the non labeled duplex (a, black) and the duplexes labeled by 3HCnt at various positions (a and b). The concentration of duplexes was 2 μ M in 20 mM PBS buffer, 50 mM NaCl, EDTA 1 mM, pH = 7.4.

Table S1. Melting temperatures of the 3HCnt-labeled duplexes

Position	Non labeled	5	7	8	9	5'	6'
T _m , °C	50	48	47	48	51	47	48
ΔT_m , °C	-	2	2	2	-1	3	2

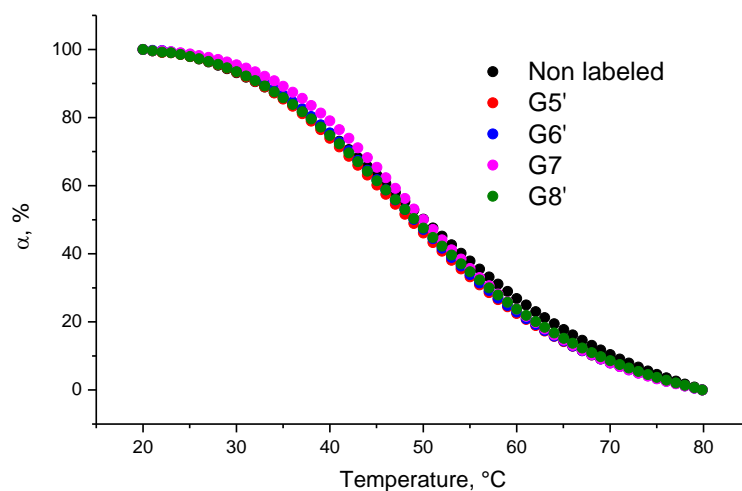


Figure S2. Thermal denaturation curves of ^3H -labeled duplexes. The curves are expressed in fraction α of strands in the duplex state versus temperature for the non labeled duplex (black) and the duplexes labeled by ^3H G at various positions. The concentration of duplexes was 2 μM in 20 mM PBS buffer, 50 mM NaCl, EDTA 1 mM, pH = 7.4.

Table S2. Melting temperatures of ^3H G-labeled duplexes

Position	Non labeled	5'	6'	7	8'
T_m , °C	50	49	49	50	49
ΔT_m , °C	-	1	1	0	1

Emission spectra of 3HCnt in free form and when incorporated in a duplex

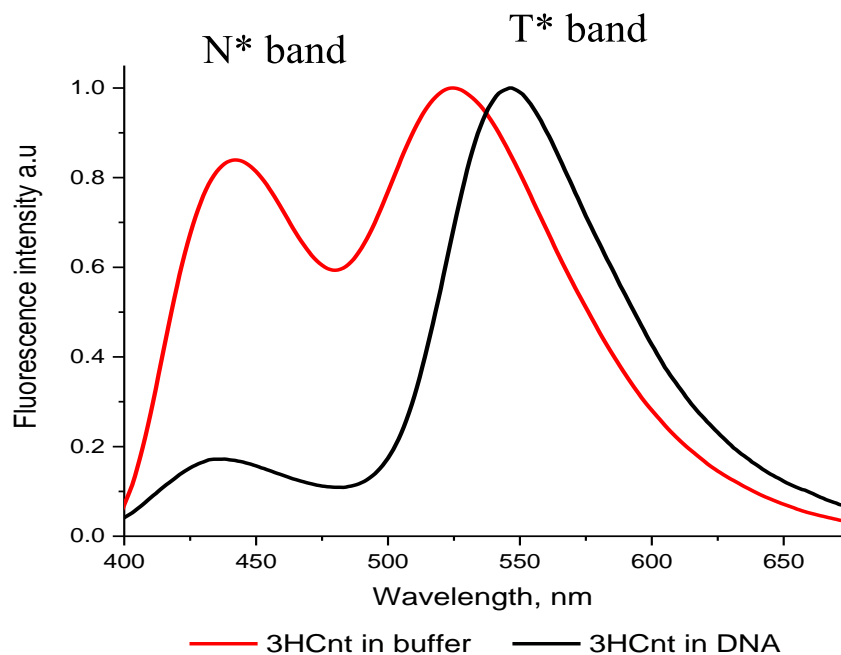


Figure S3. Fluorescence spectra of 3HCnt either free (red curve) or incorporated at position 5 in the duplex (black curve). N* (normal) and T* (tautomer) forms generate the higher and lower energy emission bands, respectively. Experiments were done in phosphate buffer 20 mM, NaCl 50 mM, TCEP 2.5 mM, 1mM EDTA, PEG 0.05%, pH 7.5, at T=20° C. The spectra were normalized at the T* band maximum.

Quantum yield of the 3HCnt-labeled duplexes

Table S3. Quantum yield and N*/T* ratio of 3HCnt-labeled DNAs in the absence and the presence of SRA¹

3HCnt position	Methylation status	QY,% DNA free ²	QY,% SRA/DNA complex ²	$\frac{QY_{SRA/DNA}}{QY_{DNAfree}}$	N*/T* DNA free	N*/T* SRA/DNA complex	$\frac{N^*/T^*_{SRA/DNA}}{N^*/T^*_{DNAfree}}$
Free 3HC		5.2			0.84		
C5	HM	1.1	4.4	3.8	0.17	0.08	0.47
	NM	1.1	3.7	3.25	0.17	0.08	0.47
G7	HM	1.1	7.4	6.5	0.14	0.05	0.36
	NM	1.1	5.7	5.0	0.14	0.06	0.44
C8	HM	0.9	1.6	1.9	0.145	0.10	0.69
	NM	0.8	0.9	1.1	0.15	0.14	0.93
A9	HM	2.1	2.6	1.3	0.11	0.10	0.91
	NM	2.0	2.6	1.3	0.115	0.10	0.87
G5'	HM	0.5	1.3	2.6	0.19	0.06	0.32
	NM	0.5	0.7	1.4	0.19	0.14	0.74
G6'	HM	1.8	4.6	2.6	0.12	0.06	0.50
	NM	1.8	4.1	2.27	0.12	0.06	0.50

¹Values are average of five experiments. Standard deviations are equal or less than 20 %,

²Quantum yields for labeled DNA were calculated using quinine sulfate (QY=0.546 in 0.5 M H₂SO₄) as a reference.

Quantum yield of thG-labeled duplexes

Table S4. Quantum yields of thG-labeled DNAs in the absence and the presence of SRA¹

th G position	Methylation status	QY,% DNA free ²	QY,% SRA/DNA complex ²	$\frac{QY_{SRA/DNA}}{QY_{DNAfree}}$
Free th G		46		
G5'	HM	8.2	10.8	1.3
	NM	8.5	9.3	1.1
G6'	HM	7.2	8.6	1.2
	NM	6.9	7.6	1.1
G7	HM	7.3	23.4	3.2
	NM	7.1	11.4	1.6
G8'	HM	7.8	11.7	1.5
	NM	7.5	9.1	1.2

¹Values are average of five experiments. Standard deviations are equal or less than 20 %,

²Quantum yields of labeled DNAs were calculated using quinine sulfate (QY=0.546 in 0.5 M H₂SO₄) as a reference.

Binding of SRA to the non labeled HM duplex, as monitored by ITC

The binding of SRA with the non-labeled HM duplex was characterized by ITC. The binding reaction was found exothermic (Fig. S4a), showing a 1:1 stoichiometry and an apparent affinity constant, $K_{app} = 5.3(\pm 0.7)\times 10^6 \text{ M}^{-1}$ (Fig. S4b), in good agreement with the values in the literature^{21,24}.

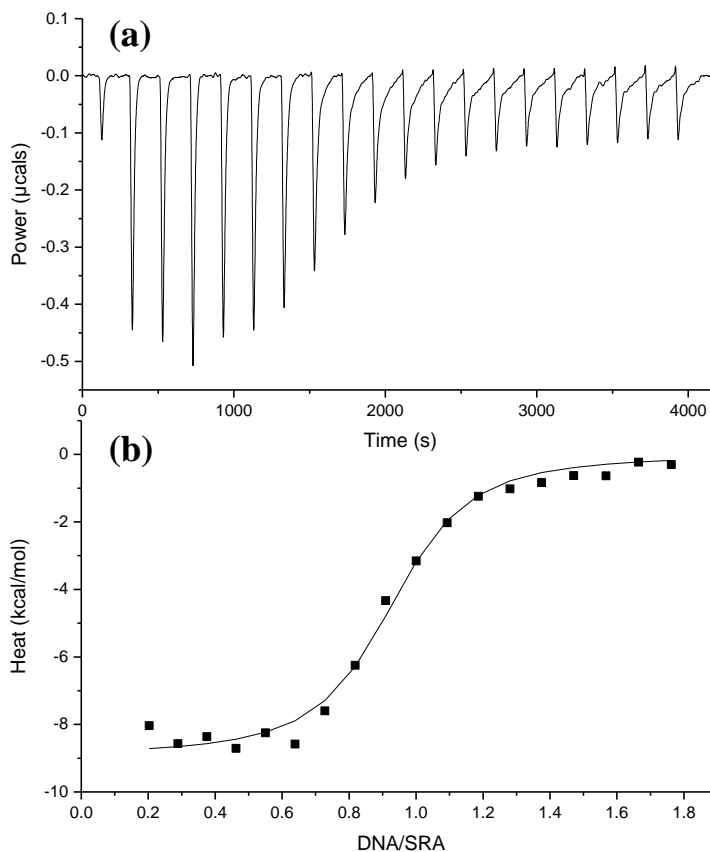


Figure S4. Binding of SRA to non-labeled HM duplex, as monitored by ITC. Heat release as a function of the injection time (a) and the DNA/SRA molar ratio (b). The solid line corresponds to the fit with a 1:1 binding model and an apparent binding constant of $5.3(\pm 0.7)\times 10^6 \text{ M}^{-1}$.

Binding of SRA and its G448D mutant to the 3HCnt/thG-labeled duplexes

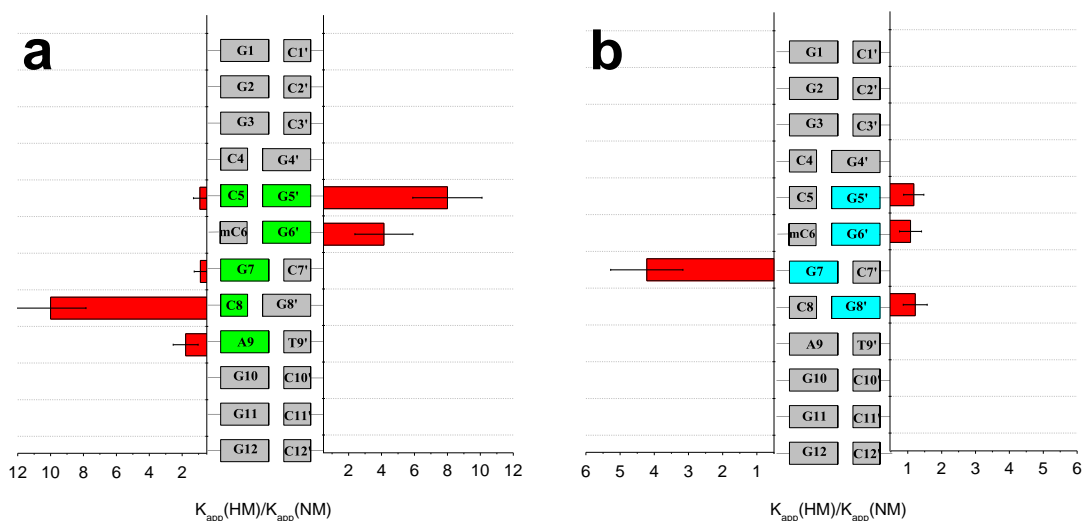


Figure S5. Effect of C6 methylation on the affinity constants of SRA to the duplexes. At each position, the ratio of the K_{app} value for HM duplex to that for NM duplex is given for (a) 3HCnt- and (b) thG-labelled duplexes. Buffer was as in Fig. S3.

N*/T* ratio of the 3HCnt-labeled duplexes

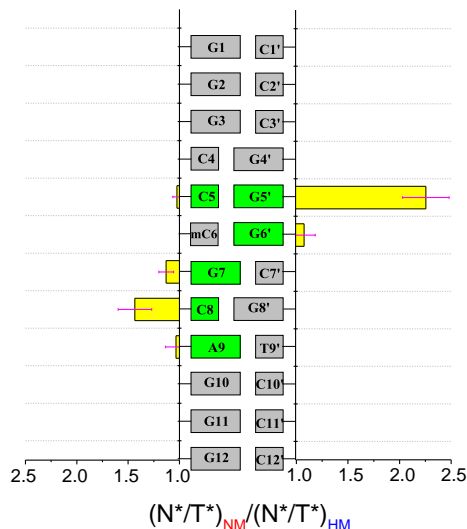


Figure S6. SRA-induced changes in the N*/T* ratio of 3HCnt-labeled duplexes. The N*/T* ratio changes were calculated by dividing the N*/T* ratio value of 3HCnt in the SRA/NM-duplex complex to that of 3HCnt in the SRA/HM-duplex. Concentration of labeled duplexes was 1 μ M, while the SRA concentrations were chosen to complex 80% of the DNA molecules (Table S5). Data are expressed as means \pm standard deviation for five independent experiments. The buffer was as in Fig. S3.

Table S5. Concentrations of SRA and its G448D mutant used to ensure 80% binding to the 3HCnt-labeled duplexes

3HCnt position	Methylation status of C6	C _{SRA} (for 1 μ M DNA), μ M	C _{SRA} (for 0.3 μ M DNA), μ M	C _{G448D} (for 1 μ M DNA), μ M	C _{G448D} (for 0.3 μ M DNA), μ M
C5	HM	1			
	NM	1			
G7	HM	1.5			
	NM	1.4			
C8	HM	2.4	1.9	17.5	17
	NM	8.1	7.7	32	31
A9	HM	3			
	NM	4.8			
G5'	HM	2.5	2.0	22	21
	NM	15	14.5	23	22
G6'	M	1			
	NM	1.3			

The concentrations of SRA and its G448D mutant were calculated using the K_{app} values of Fig. 2c.

Table S6. Concentrations of SRA and its G448D mutant used to ensure 80% binding to the thG-labeled duplexes

3HCnt position	Methylation status of C6	C _{SRA} (for 1 μ M DNA), μ M	C _{SRA} (for 0.3 μ M DNA), μ M	C _{G448D} (for 1 μ M DNA), μ M	C _{G448D} (for 0.3 μ M DNA), μ M
G5'	HM	3			
	NM	3.5			
G6'	HM	3.2			
	NM	3.5			
G7	HM	1.3	0.7	8	7
	NM	2.5	2	12	10
G8'	HM	2.5			
	NM	3.1			

The concentrations of SRA and its G448D mutant were calculated using the K_{app} values of Fig. 2d.

Stopped flow kinetics study of G448D SRA mutant with HM and NM duplexes labeled with ^3H Cnt or ^3H G

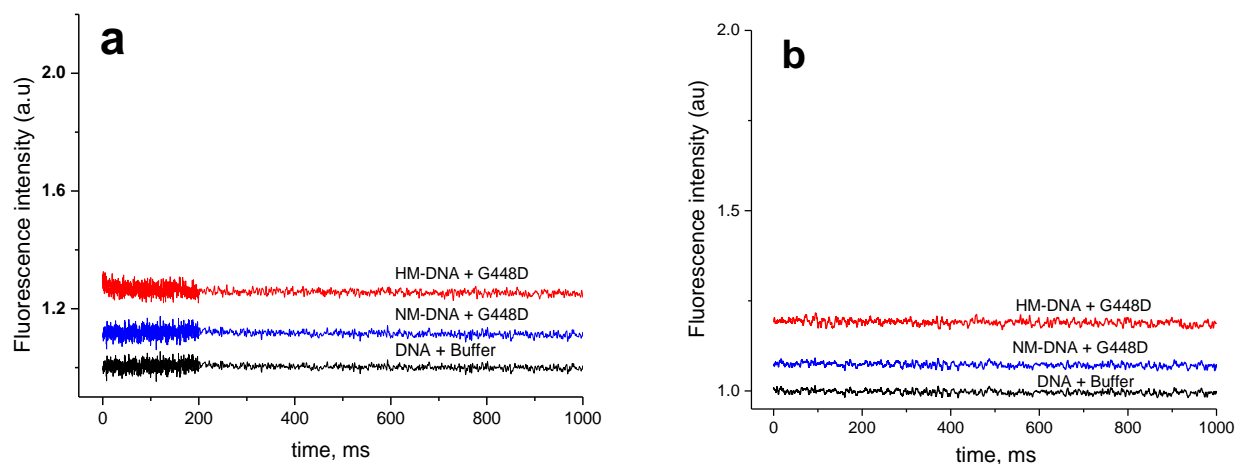


Figure S7. Interaction kinetics of G448D SRA mutant with HM and NM duplexes, as monitored by stopped-flow. Kinetic traces were obtained with duplexes labeled by ^3H Cnt at position 8 (a) or by ^3H G at position 7 (b). The black traces correspond to HM- or NM-duplexes mixed with the buffer. The blue and red kinetic traces describe the interaction of G448D SRA mutant with NM- and HM-duplexes, respectively. The fast jump in the fluorescence signal for HM and NM DNA is attributed to the binding of DNA to SRA mutant G448D. The absence of slow kinetics component for HM DNA confirms the absence of base flipping with the SRA G448D mutant. The concentration of duplexes was $0.3 \mu\text{M}$, while the concentrations of protein were chosen to ensure 80% of binding (Table S5 and S6). Experiments were done in phosphate buffer 20 mM, NaCl 50 mM, 2.5 mM TCEP, 1 mM EDTA, PEG 0.05%, pH 7.5, at $T=20^\circ \text{C}$.

NMR experiments performed on a model DNA dodecamer with 3HCnt in central position.

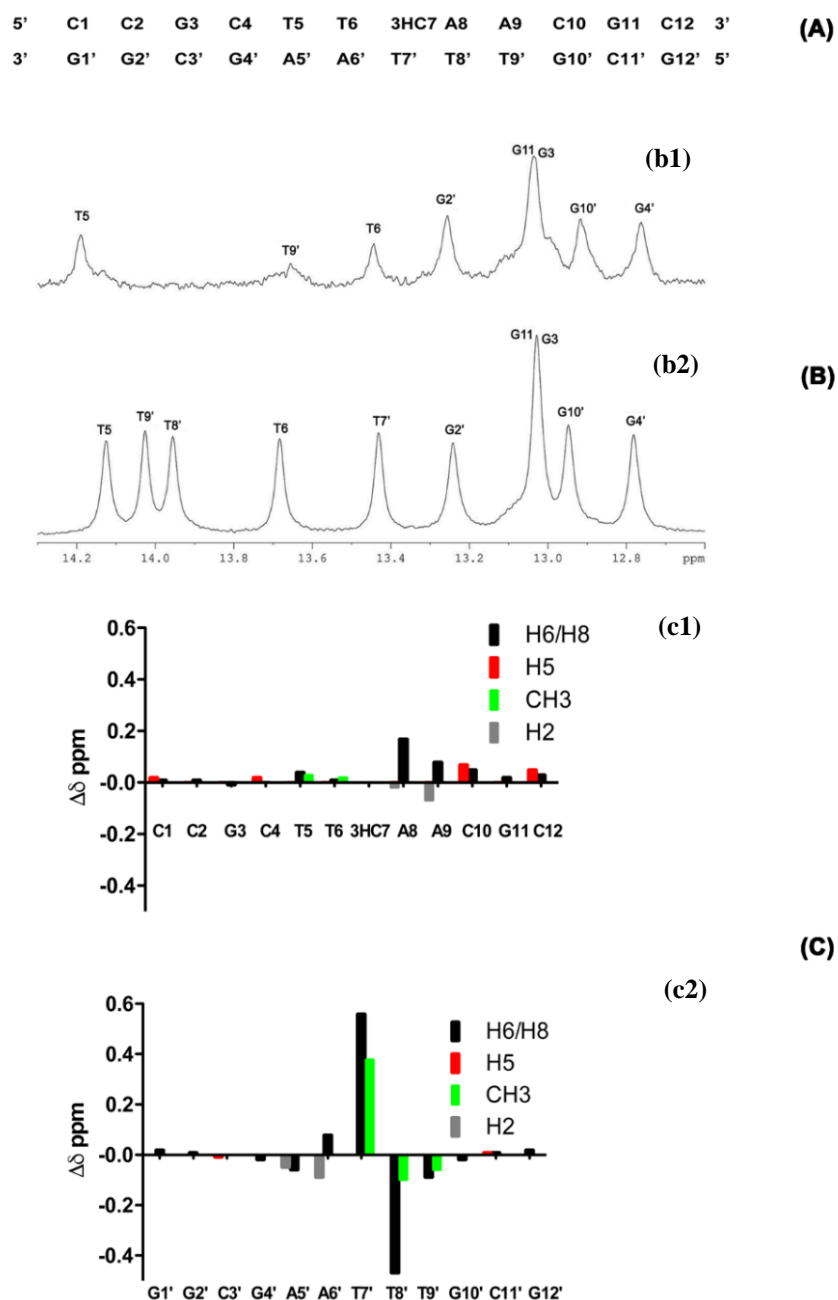


Figure S8. ^1H NMR of a model duplex labelled with 3HCnt. (A) Sequence of the model DNA duplex with 3HCnt inserted at 7th position of one of the strands. (B) Imino region of the ^1H NMR 1d spectra of (b1) the modified dodecamer and (b2) the unmodified dodecamer with a thymine at the 7th position. The imino proton resonances are labeled with the name of the residue bearing the imino proton (either G or T). The largest perturbations of the base pairing are observed for T7' and T8' for which the imino protons are not observed and at a lesser degree for T9' that is significantly broadened. These base pairs correspond to those of the insertion site (position n) and the n + 1, n + 2 base pairs in the 3' direction to the 3HCnt. (C) Difference of the aromatic proton chemical shifts ($\Delta\delta$) between the modified and the

unmodified dodecamers. H6 stands for the H6 proton of pyrimidines, H8 for the H8 proton of purines, H2 for the H2 proton of adenines and CH3 for the methyl protons CH3 of thymine; (c1) upper strand bearing the 3HCnt insertion; (c2) the complementary strand. The largest perturbations are localized at the insertion site (n site) and at the $n + 1$ and $n + 2$ base pairs.